Contents lists available at Science-Gate

International Journal of Advanced and Applied Sciences

Journal homepage: http://www.science-gate.com/IJAAS.html

Dynamics of dark solitons in optical fibers governed by cubic-quintic discrete nonlinear Schrödinger equations

Haves Qausar [1], Marwan Ramli [2,*], Said Munzir [2], Mahdhivan Syafwan [3]

[1]*Graduate School of Mathematics and Applied Sciences, Universitas Syiah Kuala, Banda Aceh 23111, Indonesia*
[2]*Department of Mathematics, Faculty of Mathematics and Natural Sciences, Universitas Syiah Kuala, Banda Aceh 23111, Indonesia*
[3]*Department of Mathematics, Universitas Andalas, Padang 25163, Indonesia*

ARTICLE INFO

Article history:
Received 17 July 2023
Received in revised form
23 December 2023
Accepted 30 October 2024

Keywords:
Dark solitons
Optical fibers
Energy distribution
Attenuation effects
Hamiltonian dynamics

ABSTRACT

This study investigates the dynamics of dark solitons and energy distribution in electromagnetic waves propagating through optical fibers, focusing on the impact of key parameters on energy retention. While previous research has emphasized frequency and dispersion, this work also examines the effect of attenuation on soliton behavior. The energy distribution is analyzed using Hamiltonian dynamics derived from the cubic-quintic discrete nonlinear Schrödinger (CQ DNLS) equation, with stationary solutions obtained via the Trust Region Dogleg method and the fourth-order Runge-Kutta (RK4) method used for dynamic simulations. Results reveal that frequency and dispersion parameters enhance wave amplitude and energy, whereas high attenuation significantly reduces wave intensity and energy during propagation. Balancing these effects is critical for maintaining energy stability and providing insights into material selection for optical fibers with low attenuation properties.

1. Introduction

The rapid expansion of information in the modern era has created a significant strain on the communication infrastructure. To address this issue and satisfy the information needs of society, optical fiber technology has emerged and evolved to handle large volumes of data with high speed and capacity (Qi et al., 2022). Despite its benefits, the transmission of information through optical fiber encounters challenges in the form of dispersion and nonlinear effects (Biondini and Lottes, 2019; Wang et al., 2019). These factors limit the speed at which information can be transmitted. However, the equilibrium between dispersion and nonlinear effects can give rise to solitons, which are optical pulses that can effectively overcome these limitations (Song et al., 2019; Ozisik, 2022).

In terms of its physicality, a soliton refers to a solitary wave that exists independently and possesses wave-particle duality. It is capable of preserving its shape and velocity while propagating through the medium (Syafwan and Arifin, 2018). Solitons found in fiber lasers are categorized into two types: Bright and dark solitons. Bright solitons are characterized by strong peaks on a weak background in the anomalous group-velocity dispersion regime of fibers. On the other hand, dark solitons are the dips on a strong background in the normal group-velocity dispersion regime of fibers (Hosseini et al., 2022; Zhao et al., 2020).

Dark soliton possesses distinct characteristics from the bright soliton. The formation of dark solitons in fiber optics is due to the nonlinearity of the medium. This nonlinearity leads to a phenomenon known as self-phase modulation (SPM), where the phase of the light changes due to its own intensity. When light with a specific frequency and amplitude is launched into an optical fiber, SPM can cause a phase shift of 180 degrees in the light, resulting in a dark soliton (Tang et al., 2014; Zhao and Li, 2022). In comparison to the bright soliton, the dark soliton has a longer transmission distance, a slower pulse broadening speed, and is more stable and resilient to various perturbations such as fiber loss (Liu et al., 2019; Wang et al., 2021), Raman scattering (Abdel-Gawad, 2021), and interaction of soliton (Yan and Chen, 2022; Wang et al., 2022). The dark soliton offers a greater coding rate and improved self-repair

* Corresponding Author.
Email Address: marwan.math@unsyiah.ac.id (M. Ramli)
https://doi.org/10.21833/ijaas.2024.11.015
Corresponding author's ORCID profile:
https://orcid.org/0000-0003-1225-9063

capability, especially for long-distance propagation. Soliton displays a more promising potential for upcoming ultra-long-distance communication systems. (Yang et al., 2022).

Through theoretical research and experimental observations, the existence of dark solitons in fiber optics has been confirmed (Baronio et al., 2018; Yao et al., 2019). Theoretically, an equation known as the Discrete Nonlinear Schrödinger equation (DNLS) (Kevrekidis, 2009) can be used to approximate soliton propagation in optical fiber. The DNLS equation is used in many different fields, such as plasma physics (Kourakis and Shukla, 2005), molecular biology (Gninzanlong et al., 2018; Okaly and Nkoa, 2022), matter waves (Bose Einstein Condensates) (Zhang et al., 2022; Jia et al., 2022), electrical lattices (Motcheyo et al., 2011), array of waveguide (Susanto and Karjanto, 2008; Efe and Yuce, 2015; Motcheyo et al., 2017), and many more. The DNLS equation in nonlinear optics can be used to observe how electromagnetic waves propagate through a single-mode optical fiber medium. The fundamental DNLS that has a dark soliton is given by

$$i\dot{\psi}_n + C\Delta\psi_n \pm F(\psi_{n+1}, \psi_n, \psi_{n-1}) = 0 \quad (1)$$

where, $\Delta\psi_n = \psi_{n+1} - 2\psi_n + \psi_{n-1}$ denotes a 1-D discrete laplacian, $\psi_n(t) : \mathbb{R}^+ \rightarrow \mathbb{C}$, $n \in \mathbb{Z}$, and C are real-valued parameters. The $\psi_n(t)$ term represents the wave function in time t on the n-th lattice and $\dot{\psi}_n(t)$ represents the derivative of the function $\psi_n(t)$ with respect to t. The $F(\psi_{n+1}, \psi_n, \psi_{n-1})$ term represents the nonlinearity term. The most commonly used nonlinear term is the cubic nonlinear form denoted by $|\psi_n|^2\psi_n$ (Kevrekidis and Carretero-González, 2009). In nonlinear optics, cubic nonlinearity is frequently referred to as Kerr nonlinearity, which refers to a certain type of material whose nonlinear refractive index change is linearly dependent on light intensity (Zanga et al., 2020). However, along with the development of research on soliton propagation, it was found that when the intensity of light passing through the optical fiber increases, the non-Kerr nonlinear effect also increases and can no longer be ignored, so that the soliton will be better if modeled by combining high-order as well as quintic nonlinearity. Therefore, the cubic-quintic DNLS (CQ DNLS) equation is used (Qausar et al., 2020).

Although the theoretical and empirical studies about dark solitons are still limited, the research related to dark solitons in the DNLS cubic-quintic equation has been conducted and evolved over the years. Maluckov et al. (2007) discussed the solution for two types of dark solitons, staggered and unstaggered, which then analyzed its stability by dividing each type into two cases, namely on-site and intersite. The study by Motcheyo et al. (2019) examined the phenomenon of supratransmission, focusing on the formation of a train of dark solitons through nonlinear gap transmission. This research builds on their findings to further explore the dynamics of dark solitons, starting with the derivation of stationary equations. The next step involves calculating the forbidden band in the dispersion relation to identify optimal frequency and dispersion values for generating dark solitons. While earlier studies primarily focused on frequency and dispersion, this research also investigates the effect of attenuation on the propagation of dark solitons in optical fibers. The key contribution of this study is to analyze how attenuation influences energy changes in electromagnetic waves, as modeled by the dynamics of dark solitons, with the goal of managing energy loss in optical fibers.

In the manufacturing process, there are often imperfections, such as radius fluctuations and variations in the lattice parameters that define the medium. This causes an optical fiber to be inhomogeneous. This non-uniformity in a real fiber's core medium influences several factors, including self-phase modulation, frequency, dispersion, and attenuation (Gao et al., 2021; Liu et al., 2019). Attenuation in nonlinear optics refers to the weakening of waves that happens as a result of the interaction between electromagnetic waves and a medium. As a consequence of attenuation in optical fibers, electromagnetic waves experience a reduction in energy while they travel through the fiber. This paper will discuss the dynamics of dark soliton and Hamiltonian distribution to analyze electromagnetic wave energy in fiber optics based on the soliton solution in the CQ DNLS equation by varying the frequency, dispersion, and attenuation. The Trust Region Dogleg method (Kimiaei, 2022; Zhang et al., 2022) will be used to determine the solution to the CQ DNLS equation, and the solution's dynamics will be observed using the 4th order Runge-Kutta method (Kartono et al., 2020; Raza et al., 2021). This paper is systematically arranged as follows. The CQ DNLS equation and methods will be introduced in the second section. The results and discussion related to this research will be presented in the third section, and the dark soliton solution obtained based on the CQ DNLS equation, stability, soliton dynamics, and Hamiltonian distribution will be presented. Finally, in the fourth section, we present our findings and conclusions in brief.

2. Materials and methods

2.1. Discrete nonlinear Schrödinger's equation with cubic-quintic nonlinearity

The DNLS equation is a difference-differential equation that can be used to explain wave propagation in a dispersive medium. In general, the DNLS equation can be expressed as follows:

$$i\dot{\psi}_n = -C(\psi_{n+1} - 2\psi_n + \psi_{n-1}) \mp F(\psi_{n+1}, \psi_n, \psi_{n-1}) \quad (2)$$

where, $\psi_n \equiv \psi_n(t) \in \mathbb{C}$ is a wave function in the $t \in \mathbb{R}^+$ and $n \in \mathbb{Z}$ domains, $\dot{\psi}_n$ represents the derivative with respect to t of the function ψ_n, C represents the dispersion parameter, F denotes a nonlinear term, and $i^2 = -1$. Nonlinear terms in the form of cubic

$|\psi_n|^2\psi_n$ and quintic $|\psi_n|^4\psi_n$ are used in this paper, so that Eq. 2 can be rewritten as follows:

$$i\dot{\psi}_n = -C(\psi_{n+1} - 2\psi_n + \psi_{n-1}) + B|\psi_n|^2\psi_n - Q|\psi_n|^4\psi_n - i\frac{\alpha}{2}\psi_n \quad (3)$$

where, B represents the coefficients of the cubic terms, Q represents the coefficients of quintic terms, and α represents the attenuation parameter in optical fiber. Eq. 3 conserves two dynamical invariants: Norm (or power, in terms of optics),

$$M = \sum_n |\psi_n|^2 \quad (4)$$

and energy (Hamiltonian),

$$H = \sum_n \left[C\overline{\psi_n}(\psi_{n+1} - 2\psi_n + \psi_{n-1}) + \frac{B}{2}|\psi_n|^4 - \frac{Q}{3}|\psi_n|^6 + i\frac{\alpha}{2}|\psi_n|^2\right]. \quad (5)$$

The stationary form of the CQ DNLS equation can be obtained by performing ansatz substitution $\psi_n = u_n e^{-iwt}$ to Eq. 3 with w indicates the frequency parameter in the real domain. In addition, the stationary form of CQ DNLS is not affected by attenuation, and without loss of generality B can be scaled out to 1, and Q can be scaled out to 0.5, by the transformation,

$$\psi_n \to \sqrt{\frac{B}{2Q}}\psi_n, \quad t \to \frac{2Q}{B^2}t, \quad C \to \frac{B^2}{2Q}C, \quad (6)$$

so that the stationary CQ DNLS equation can be written as follows:

$$wu_n + C(u_{n+1} - 2u_n + u_{n-1}) - u_n^3 + 0.5u_n^5 = 0, \quad u_n \in \mathbb{R}, \quad n = -N, -N+1, \cdots, N, \quad N \in \mathbb{Z}^+ \quad (7)$$

where, $u_{\pm(N+1)} = u_{\pm N}$. The dark soliton obtained in the stationary CQ DNLS Eq. 7 is later needed as an initial value for simulating the soliton dynamics in the CQ DNLS equation with varying attenuation effects. In addition, the dispersion relation is also needed in determining the forbidden band (Motcheyo et al., 2019) at frequency w to generate the dark soliton solution. The dispersion relation in Eq. 3 can be found by substituting $\psi_n = u_n e^{-i(kn-wt)}$ where k is the wave number into the linearized form of Eq. 3 and ignoring the attenuation effect. The linear dispersion law is obtained:

$$w = C(-2 + 2\cos(k)). \quad (8)$$

From this linear dispersion, the linear phonon band (Motcheyo and Macías-Díaz, 2023) $-4C \le w \le 0C = 0$ and the forbidden band $w < -4C$ or $w > 0. C = 0$ are known.

2.2. Method of trust region

To obtain the dark soliton solution for the stationary CQ DNLS equation, the trust region dogleg method is employed. This involves defining a system of nonlinear equations, which can be expressed mathematically as:

$$F(\boldsymbol{u}) = 0, \quad \boldsymbol{u} = (u_1, u_2, \cdots, u_m) \in \mathbb{R}^m \quad (9)$$

where, $F: \mathbb{R}^m \to \mathbb{R}^m$ is a mapping that can be expressed as $F(\boldsymbol{u}) = (F_1(\boldsymbol{u}), F_2(\boldsymbol{u}), \cdots, F_m(\boldsymbol{u}))^T$ and $n \in \{1,2, \cdots, m\}$ satisfies $F_n: \mathbb{R}^m \to \mathbb{R}^m$ is continuous and differentiable. Regarding the stationary equation DNLS Eq. 7, define the function F_n as follows:

$$F_n(\boldsymbol{u}) = wu_n + C(\psi_{n+1} - 2\psi_n + \psi_{n-1}) - u_n^3 + 0.5u_n^5 \quad (10)$$

finding a solution for $\boldsymbol{u}^*$ in Eq. 9 is the same as finding a solution to the unconstrained least squares problem

$$f(\boldsymbol{u}) = \min_{\boldsymbol{u}\in\mathbb{R}^m} \frac{1}{2}\|F(\boldsymbol{u})\|^2, \quad (11)$$

where, $\|\ .\ \|$ represents the Euclidean norm. The unconstrained least squares problem Eq. 11 can be determined using the Method of Trust Region. The Trust Region Method begins by developing a function model that can approximate F near the $\boldsymbol{u}_k \in \mathbb{R}^m$

$$M_k(\boldsymbol{u}) = F(\boldsymbol{u}_k) + J(\boldsymbol{u}_k)(\boldsymbol{u} - \boldsymbol{u}_k) \quad (12)$$

where, the Jacobian on F at the point $\boldsymbol{u}_k$ is denoted by $J(\boldsymbol{u}_k)$. Apply Eq. 11 to find a solution to the function model $M_k(\boldsymbol{u})$ so that the problem becomes:

$$m_k(u) = \min_{u\in\mathbb{R}^m} \frac{1}{2}\|M_k(u)\|^2 = \min_{u\in\mathbb{R}^m} \frac{1}{2}\|F(u_k) + J(u_k)(u - u_k)\|^2 = \min_{u\in\mathbb{R}^m} \frac{1}{2}F(u_k)^T F(u_k) + (u - u_k)^T J(u_k)^T F(u_k) + \frac{1}{2}(u - u_k)^T J(u_k)^T J(u_k)(u - u_k). \quad (13)$$

where, the gradient on F at the point $\boldsymbol{u}_k$ denoted by $J(\boldsymbol{u}_k)^T F(\boldsymbol{u}_k)$. Defines R_k as a trust region,

$$R_k = \{\boldsymbol{u} \in \mathbb{R}^m : \|\boldsymbol{u} - \boldsymbol{u}_k\| \le \Delta_k\}. \quad (14)$$

where, the trust region radius denoted by $\Delta_k \in \mathbb{R}^+$. Next, look for a vector that is in the trust region $\boldsymbol{u} \in R_k$ such that it makes $m_k(\boldsymbol{u})$ a minimum and mathematically can be written as follows:

$$\boldsymbol{v}_{k+1} = \arg\max_{u\in R_k} m_k(\boldsymbol{u}) \quad (15)$$

Eq. 15 is often called the Trust Region Sub problem (Wang et al., 2020).

2.3. Cauchy point and quasi-newton point

The Cauchy point is a point in the trust region and is in the direction of descent. Before defining the Cauchy point, note that:

$$\nabla f(\boldsymbol{u}_k) = J(\boldsymbol{u}_k)^T F(\boldsymbol{u}_k) \quad (16)$$

This results in the descent direction being along $-\alpha J(\boldsymbol{u}_k)^T F(\boldsymbol{u}_k)$ with $\alpha > 0$. In order to determine $\alpha > 0$, the Steepest Descent direction is used on m_k in $\boldsymbol{u}_k$ so that it can be written:

$$\alpha_k^u = \arg\min_{\alpha>0} m_k\left(\boldsymbol{u}_k - \alpha J(\boldsymbol{u}_k)^T F(\boldsymbol{u}_k)\right) = \frac{F(\boldsymbol{u}_k)^T J(\boldsymbol{u}_k) J(\boldsymbol{u}_k)^T F(\boldsymbol{u}_k)}{F(\boldsymbol{u}_k)^T J(\boldsymbol{u}_k) J(\boldsymbol{u}_k)^T J(\boldsymbol{u}_k) J(\boldsymbol{u}_k)^T F(\boldsymbol{u}_k)} \quad (17)$$

and the Cauchy Point can be defined as $\boldsymbol{v}_k^c = \boldsymbol{u}_k - \alpha_k^c J(u_k)^T F(\boldsymbol{u}_k)$ with $\alpha_k^c = \min\left(\frac{\Delta_k}{\|J(u_k)^T F(u_k)\|}, \alpha_k^u\right)$. Quasi-Newton points are found based on the calculation of $M_k(\boldsymbol{u}) = 0$ and can be written as $\boldsymbol{v}_k^{qn} = \boldsymbol{u}_k - J(\boldsymbol{u}_k)^{-1} F(\boldsymbol{u}_k)$ (Brust et al., 2019).

2.4. Dogleg method

In order to find a solution to the Trust Region subproblem, as in Eq. 15, Dogleg's method is used. This method is related to the Quasi-Newton point $\boldsymbol{v}_k^{qn}$ and the Cauchy point $\boldsymbol{v}_k^c$. The dogleg method will create a path Eq. 18 that passes through these two points such that the model function Eq. 13 is minimum along the path Eq. 18.

Finally, a candidate point $\boldsymbol{v}_{k+1}$ is selected which makes the model function Eq. 13 minimum on that path but is still in the trust region radius. This method is called Dogleg because it works with two lines similar to a dog's leg with the knee being the minimal point of steepest descent direction, namely $\boldsymbol{v}_k^u = \boldsymbol{u}_k - \alpha_k^u J(\boldsymbol{u}_k)^T F(\boldsymbol{u}_k)$ and continuing to the Quasi-Newton point $\boldsymbol{v}_k^{qn}$ through the dogleg path defined as follows:

$$\boldsymbol{v}(\tau) = \begin{cases} \boldsymbol{u}_k + \tau(\boldsymbol{v}_k^u - \boldsymbol{u}_k) & \text{for } \tau \in [0,1], \\ \boldsymbol{v}_k^u + (\tau - 1)(\boldsymbol{v}_k^{qn} - \boldsymbol{v}_k^u) & \text{for } \tau \in [1,2]. \end{cases} \quad (18)$$

2.5. Runge-Kutta 4th order

The 4th Order Runge-Kutta method can be applied by transforming the CQ DNLS equation into the form,

$$\boldsymbol{y}_{i+1} = \boldsymbol{y}_i + \frac{1}{6}(\boldsymbol{k}_1 + 2\boldsymbol{k}_2 + 2\boldsymbol{k}_3 + \boldsymbol{k}_4)h, \qquad i = 0,1,2, \ldots \quad (19)$$

by using ODE in Eq. 19, the RK4 method (Ahmadianfar et al., 2021) can be used, with,

$$\boldsymbol{k}_1 = f(\boldsymbol{y}_i), \quad \boldsymbol{k}_2 = f\left(\boldsymbol{y}_i + \tfrac{1}{2}\boldsymbol{k}_1 h\right), \quad \boldsymbol{k}_3 = f\left(\boldsymbol{y}_i + \tfrac{1}{2}\boldsymbol{k}_2 h\right), \quad \boldsymbol{k}_4 = f\left(\boldsymbol{y}_i + \tfrac{1}{2}\boldsymbol{k}_3 h\right). \quad (20)$$

3. Results and discussion

The RK4 method was applied to analyze the behavior of dark solitons, which represent the propagation of electromagnetic waves in optical fibers. The stationary solution of the CQ DNLS equation, determined using the Trust Region Dogleg Method, served as the input signal. Changes in energy during electromagnetic wave propagation were examined by monitoring variations in Hamiltonian dynamics. The dynamics of the dark soliton and the Hamiltonian changes were influenced by parameters such as frequency, dispersion, and attenuation. Since the parameters in this study are dimensionless, the results presented are unitless.

3.1. Stationary solutions of cubic-quintic discrete nonlinear Schrödinger's equation

In the process of finding the dark soliton solution, it is necessary to form a model function by considering the dimensions of the problem Eq. (7). This causes $F(\boldsymbol{u}) = (F_{-N}(\boldsymbol{u}), F_{-N+1}(\boldsymbol{u}), \cdots, F_N(\boldsymbol{u}))^T$ with $\boldsymbol{u} = (u_{-N}, u_{-N+1}, \cdots, u_N) \in \mathbb{R}^{2N+1}$ and also makes Eq. 9 and Eq. 10 become a nonlinear system with $2N + 1$ equations, which can be expressed as follows:

$$F(\boldsymbol{u}) = \begin{bmatrix} F_{-N}(\boldsymbol{u}) \\ F_{-N+1}(\boldsymbol{u}) \\ \vdots \\ F_{-1}(\boldsymbol{u}) \\ F_0(\boldsymbol{u}) \\ F_1(\boldsymbol{u}) \\ \vdots \\ F_{N-1}(\boldsymbol{u}) \\ F_N(\boldsymbol{u}) \end{bmatrix} = \begin{bmatrix} wu_{-N} + C(u_{-N+1} - 2u_{-N} + u_{-N-1}) - u_{-N}^3 + 0.5u_{-N}^5 \\ wu_{-N+1} + C(u_{-N+2} - 2u_{-N+1} + u_{-N}) - u_{-N+1}^3 + 0.5u_{-N+1}^5 \\ \vdots \\ wu_{-1} + C(u_0 - 2u_{-1} + u_{-2}) - u_{-1}^3 + 0.5u_{-1}^5 \\ wu_0 + C(u_1 - 2u_0 + u_{-1}) - u_0^3 + 0.5u_0^5 \\ wu_1 + C(u_2 - 2u_1 + u_0) - u_1^3 + 0.5u_1^5 \\ \vdots \\ wu_{N-1} + C(u_N - 2u_{N-1} + u_{N-2}) - u_{N-1}^3 + 0.5u_{N-1}^5 \\ wu_N + C(u_{N+1} - 2u_N + u_{N-1}) - u_N^3 + 0.5u_N^5 \end{bmatrix} = \mathbf{0} \quad (21)$$

and construct the Jacobian matrix at $\boldsymbol{u}_k$ as follows:

$$J(\boldsymbol{u}_k) = \begin{bmatrix} \frac{\partial F_{-N}(\boldsymbol{u}_k)}{\partial u_{-N}} & \frac{\partial F_{-N}(\boldsymbol{u}_k)}{\partial u_{-N+1}} & \cdots & \frac{\partial F_{-N}(\boldsymbol{u}_k)}{\partial u_N} \\ \frac{\partial F_{-N+1}(\boldsymbol{u}_k)}{\partial u_{-N}} & \frac{\partial F_{-N+1}(\boldsymbol{u}_k)}{\partial u_{-N+1}} & \cdots & \frac{\partial F_{-N+1}(\boldsymbol{u}_k)}{\partial u_N} \\ \vdots & & & \vdots \\ \frac{\partial F_N(\boldsymbol{u}_k)}{\partial u_{-N}} & \frac{\partial F_N(\boldsymbol{u}_k)}{\partial u_{-N+1}} & \cdots & \frac{\partial F_N(\boldsymbol{u}_k)}{\partial u_N} \end{bmatrix} \quad (22)$$

moreover, for all $i, j \in [-N, N]$ applies,

$$\frac{\partial F_i(\boldsymbol{u}_k)}{\partial u_j} = \begin{cases} w - 2C - 3u_i^2 + 2.5u_i^4\big|_{u=u_k} & \text{if } j = 1, \\ C & \text{if } j = i-1 \text{ or } j = i+1, \\ 0 & \text{others.} \end{cases} \tag{23}$$

So that the function models Eq. 12 and Eq. 13 can be formed based on Eq. 21-22. The starting point to build the solution is to solve the anti-continuum limit case, causing the value of C to be zero. In the case of CQ DNLS, replacing $C = 0$, Eq. 24 becomes,

$$F(\boldsymbol{u}) = \begin{bmatrix} F_{-N}(u) \\ F_{-N+1}(u) \\ \vdots \\ F_{N-1}(u) \\ F_N(u) \end{bmatrix} = \begin{bmatrix} wu_{-N} - u_{-N}^3 + 0.5u_{-N}^5 \\ wu_{-N+1} - u_{-N+1}^3 + 0.5u_{-N+1}^5 \\ \vdots \\ wu_{N-1} - u_{N-1}^3 + 0.5u_{N-1}^5 \\ wu_N - u_N^3 + 0.5u_N^5 \end{bmatrix} = \mathbf{0} \tag{24}$$

Solving the system of Eq. 24 can be done by finding solutions for each F_n. This is because any two F_n have no variables related to each other. Rewrite as follows:

$$wu_n - u_n^3 + 0.5u_n^5 = 0 \tag{25}$$

and the solutions that satisfy Eq. 25 are $u_n = 0$ and $u_n = \pm\sqrt{1 \pm \sqrt{1-2w}}$. Note that the value of $u_n \in \mathbb{R}$, therefore the value of w is satisfied only in the interval $w \leq 0.5$. Based on the results obtained, two fixed points can be constructed,

$$u_n = \begin{cases} u_i = -\sqrt{1+\sqrt{1-2w}}, & i = -N, -N+1, \cdots, -1 \\ u_0 = 0, \\ u_j = \sqrt{1+\sqrt{1-2w}}, & j = 1, 2, \cdots, N. \end{cases} \tag{26}$$

$$u_n = \begin{cases} u_i = -\sqrt{1-\sqrt{1-2w}}, & i = -N, -N+1, \cdots, -1 \\ u_0 = 0, \\ u_j = \sqrt{1-\sqrt{1-2w}}, & j = 1, 2, \cdots, N. \end{cases} \tag{27}$$

In the case of the coupling constant between two adjacent lattices is not neglected, or in other words, if the value of C is not equal to zero, then an exact solution cannot be found. Therefore, the Trust Region Dogleg method is used to determine a solution. To perform the simulation, an initial value that matches the characteristics of the solution you want to find is needed. In this case, the initial value of $\tanh(n)$ is used because the dark soliton solutions have a shape that resembles the hyperbolic function. Simulations are carried out with $n = -N, -N+1, \cdots, N$ with $N \in \mathbb{Z}^+$ and divided into four categories as follows:

1. $C > 0$ and $w \leq 0$
2. $C > 0$ and $w \geq 0$
3. $C < 0$ and $w \leq 0$
4. $C < 0$ and $w \geq 0$ (28)

Based on the simulations carried out in categories 1 and 3, the solution obtained did not form a soliton solution as expected. Only in category 2 and 4 dark soliton solutions were found. Specifically, in the following intervals:

$$C \in [-0.05, 0) \cup (0, 0.94] \text{ and } w \in [0.01, 0.89]. \tag{29}$$

Although the dark soliton in Eq. 7 is formed using the parameter value Eq. 29, it should be noted that the shape of the soliton obtained is different. This depends on the magnitude of the values of w and C given. Therefore, to see the effect of parameters w and C, a plot of the dark soliton was carried out by setting a fixed parameter value and allowing the other parameters to change with constant differences. Fig. 1 represents a profile solution for dark soliton by setting the parameter $w = 0.36$ and some C values using the Trust Region Dogleg method. From Figs. 1a-1d, it can be seen that initially, the resulting solution did not form a dark soliton and also note that the C parameter used does not meet the condition Eq. 29. It can be seen in more detail for Figs. 1a-1d, sites on the right $\{u_n | n = 1, 2, \cdots, N\}$ and left $\{u_n | n = -N, -N+1, \cdots, -1\}$ still fluctuates like a sinusoidal wave with a large enough amplitude, which is about one-third of the difference between the highest u_n sites and the lowest u_n sites. Then slowly the amplitude of the wave decreases but the quantity becomes more numerous than before until finally, the wave-like fluctuation behavior on the left and right sites disappears and a dark soliton is formed, as shown in Figs. 1e-1f. If it is reviewed in more detail regarding Figs. 1e-1f, the effect of increasing the value of C, results in a decrease in position at sites u_1 and an increase in position at sites u_{-1}. In addition, the increase in the value of C did not affect the soliton height in dark soliton.

Fig. 2 represents a profile solution for dark soliton by setting parameter $C = 0.2$ and some w values using the Trust Region Dogleg method. According to Figs. 2a-2f, decreasing the value of the parameter w in the dark soliton solution resulted in a gradual increase in height at the right u_n sites and a gradual decrease in height at the left $u_n$sites up to 1 and -1, respectively.

3.2. Dark soliton stability

Once the dark soliton solution determined based on the stationary CQ DNLS equation is obtained, its stability will be examined using the linearization ansatz $u_n(t) = u_n + \delta\epsilon_n(t)$, $\delta \ll 1$. By writing $\epsilon_n = (\eta_n + i\xi_n)e^{\lambda t}$, the eigenvalue problem is obtained as follows:

$$\begin{pmatrix} 0 & -C\Delta - u_n^2 + 0.5u_n^4 \\ C\Delta + 3u_n^2 - 2.5u_n^4 & 0 \end{pmatrix} \begin{pmatrix} \eta_n \\ \xi_n \end{pmatrix} = \lambda \begin{pmatrix} \eta_n \\ \xi_n \end{pmatrix}. \tag{30}$$

Solving the eigenvalue problem Eq. 30 to get $Re(\lambda)$ and $Im(\lambda)$ so that the stability spectrum can be described.

Fig. 3 shows the spectrum of the eigenvalues for dark soliton with parameter $w = 0.36$ fixed and some C values. In general, the eigenvalues obtained are spread on the negative and positive sides of real numbers. The increasing value of C causes the eigenvalues to shift from the negative to the positive side, but almost all of them still have eigenvalues on the positive side of the real numbers, indicating that the dark soliton is unstable. The opposite is shown in Fig. 3f, where all of the eigenvalues are on the negative side of the real numbers, indicating that the resulting dark solution is stable.

Fig. 4 represents the spectrum of the eigenvalues for dark soliton with parameter $C = 0.2$ fixed and some w values. In general, the resulting eigenvalues are all on the positive side, except in Figs. 4c-4f, there is one eigenvalue that is on the negative side of the real part. Because there is no single spectrum where all eigenvalues are on the negative side of real numbers, the resulting dark soliton is unstable.

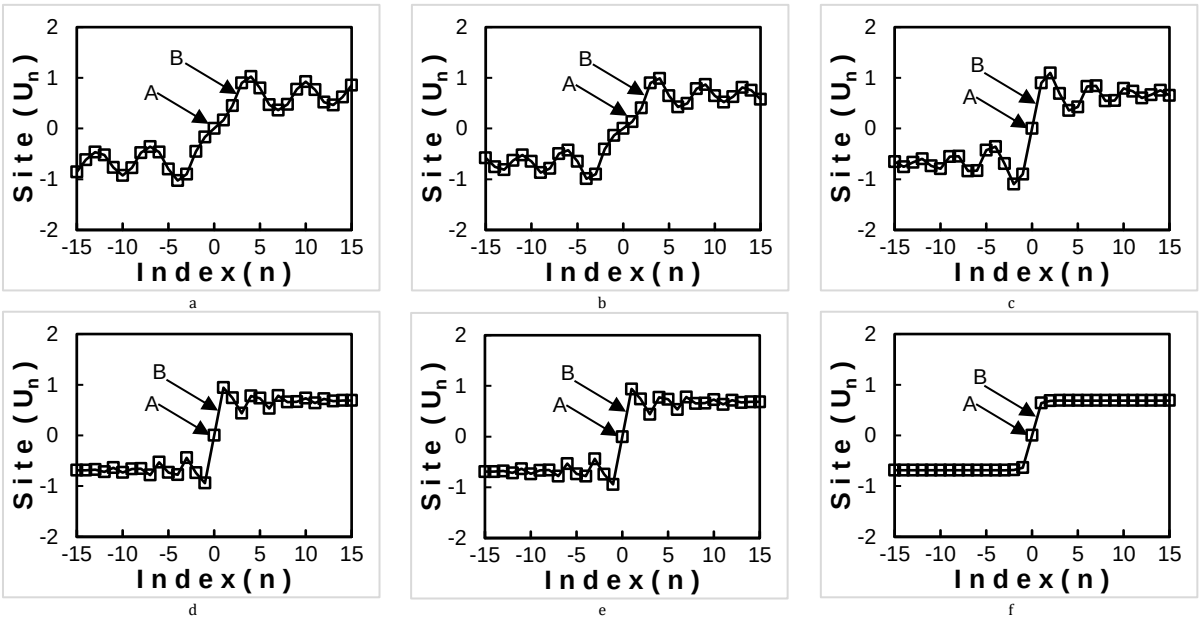

Fig. 1: Profiles solutions for dark soliton with parameter w = 0.36 fixed and some values C (a) C = −0.41 (b) C = −0.32 (c) C = −0.23 (d) C = −0.14 (e) C = −0.05 (f) C = 0.04. The n-th site is represented by the square marker indicated by arrow A, and the line connecting two adjacent sites is represented by arrow B

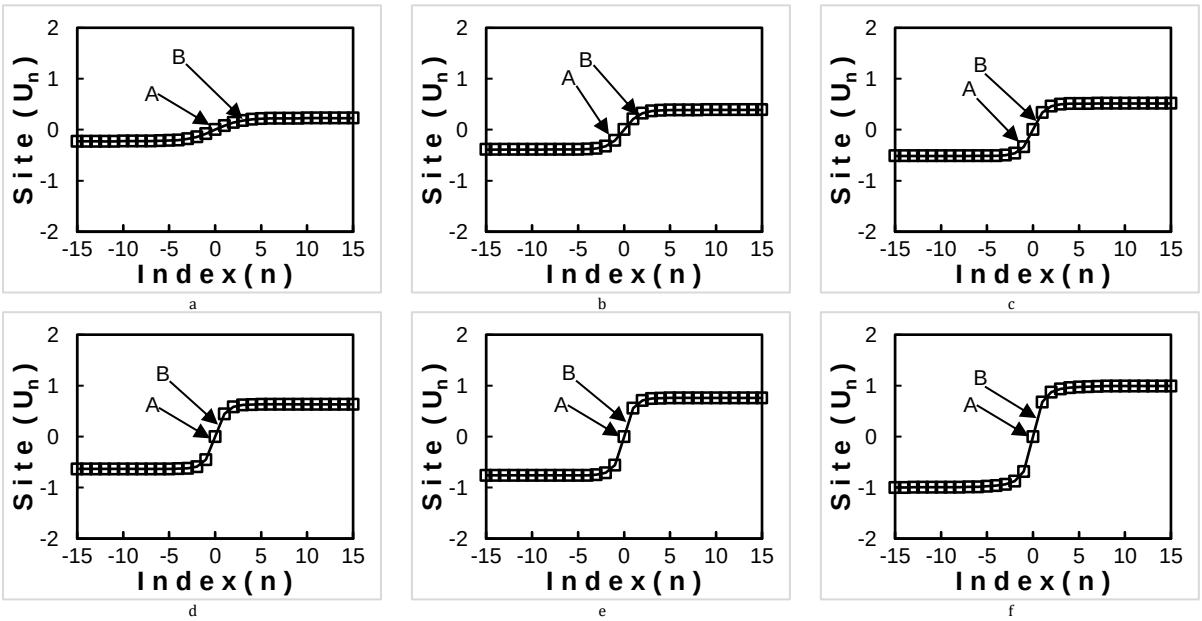

Fig. 2: Profiles solutions for dark soliton with fixed parameter C = 0.2 and some w values (a) w = 0.05 (b) w = 0.14 (c) w = 0.23 (d) w = 0.32 (e) w = 0.41(f) w = 0.5. The n-th site is represented by the square marker indicated by arrow A, and the line connecting two adjacent sites is represented by arrow B

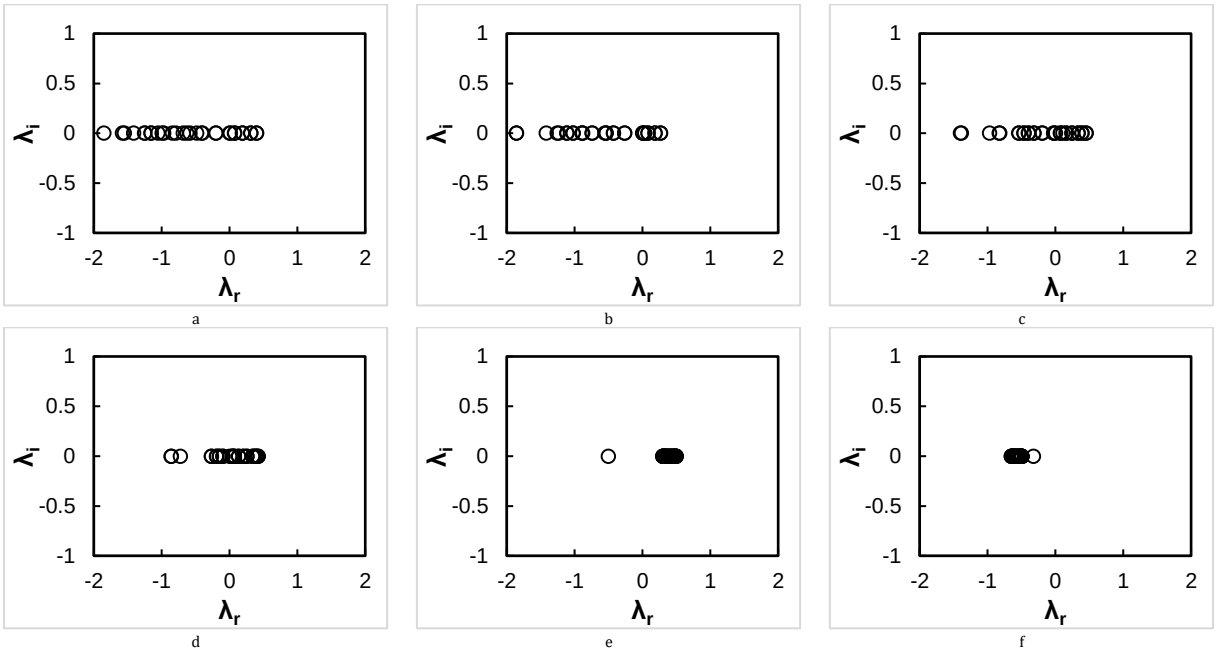

Fig. 3: The spectrum of the eigenvalues for dark soliton with parameter w = 0.36 fixed and some values C (a) C = −0.41 (b) C = −0.32 (c) C = −0.23 (d) C = −0.14 (e) C = −0.05 (f) C = 0.04

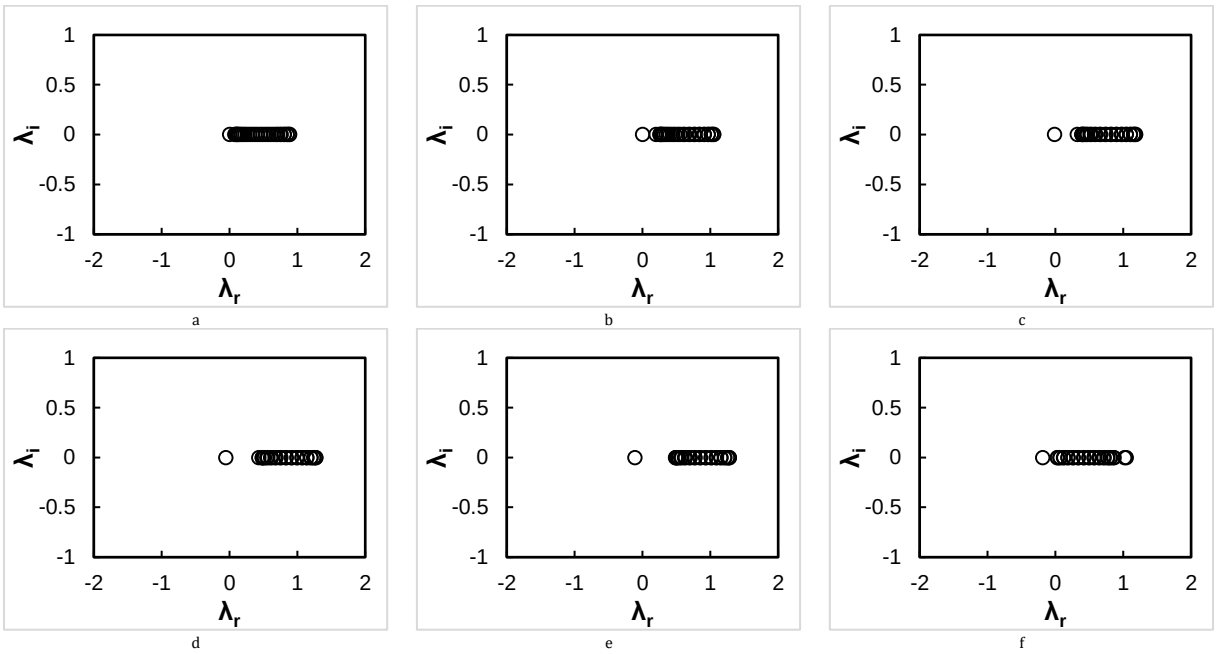

Fig. 4: The spectrum of the eigenvalues for dark soliton with parameter C = 0.2 fixed and some values w (a) w = 0.05 (b) w = 0.14 (c) w = 0.23 (d) w = 0.32 (e) w = 0.41 (f) w = 0.5

Fig. 5a shows the dark soliton's stability region on the (C, w) plane simulated along the interval (29). The color of each point in Fig. 5 represents the maximum value of the real part of the eigenvalue in each parameter C and w. It can be seen that the larger the maximum eigenvalue is, the brighter the color, while the smaller the maximum eigenvalue is, the darker the color. A stable dark soliton is characterized by a negative maximum eigenvalue, which means that the image is marked with black pixels. Then, switching to Fig. 5b, it can be seen that there are white dots in the area marked with a dark color and then move along the C axis. These are the points that are expected to be used as parameter representations in the case of fixed w and different C in simulating the differences in the dark soliton dynamics' characteristics. Similarly, in Fig. 5c, it can be seen that there are white dots in the area marked with dark color and then move along the w axis. These points will be used to represent the parameters in the case of C fixed and different w when simulating the various characteristics of the dark soliton dynamics. It is important to note that six points are selected for each case: three from the stable region and three from the unstable region.

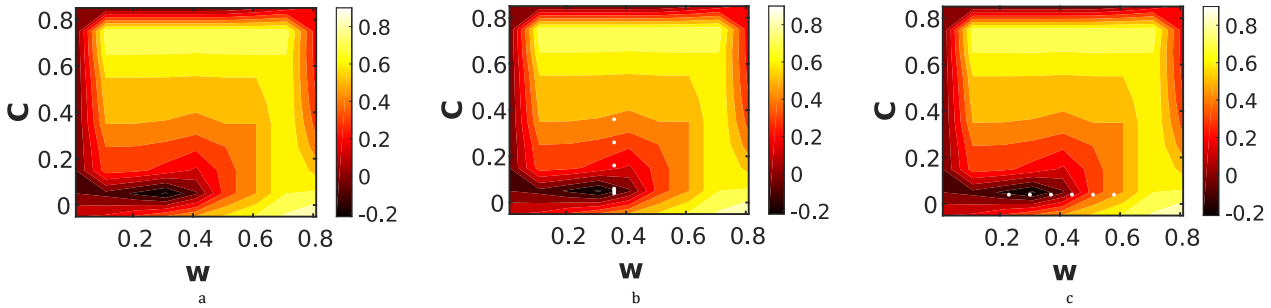

Fig. 5: The dark soliton's stability region on the (C, w) plane

3.3. Dark soliton dynamics of cubic-quintic discrete nonlinear Schrödinger's equation

The RK4 method is used to simulate dark soliton dynamics in the CQ DNLS equation by varying the frequency (w), dispersion (C), and attenuation (α) parameters in order to investigate the properties of electromagnetic waves when they interact with optical fiber.

Fig. 6 illustrates the dynamics of dark soliton in the CQ DNLS equation with $w = 0.36$ fixed and several C parameters. Based on the simulation results shown in Fig. 6 (top), the electromagnetic wave propagating along the fiber optics can maintain its shape when the parameters used are in the stable region. Conversely, Fig. 6 (bottom) shows that if the parameters used are in the unstable region, the electromagnetic wave experiences a shift so that it can no longer maintain its shape when propagating along the fiber optics. Furthermore, the C parameter influences electromagnetic wave propagation on fiber optics. A relatively large value of C causes the electromagnetic wave pulse to widen.

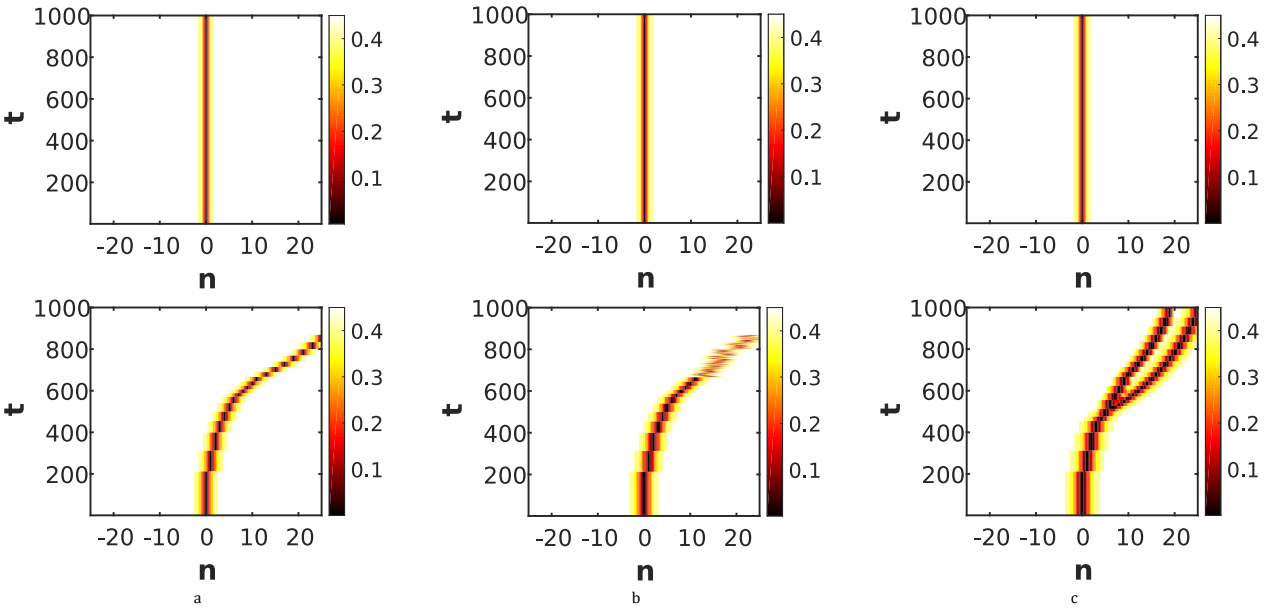

Fig. 6: Dark soliton dynamics in the CQ DNLS equation with w = 0.36 fixed and several parameters C (top) (a) C = 0.04, (b) C = 0.05, (c) C = 0.06 (bottom) (a) C = 0.16, (b) C = 0.26, (c) C = 0.36

Fig. 7 illustrates the dynamics of dark soliton in the CQ DNLS equation with $C = 0.04$ fixed and several parameters w. According to the results shown in Fig. 7, it can be seen that the value of w has a significant impact on the condition of electromagnetic waves propagating on the fiber optic. The amplitude of the electromagnetic wave increases as w increases. The electromagnetic wave can also maintain its shape while propagating in the fiber optics, as shown in Fig. 7 (top). This is because the parameters used are in a stable region of the (C, w) plane. In contrast, if the parameters are chosen in the unstable region in the (C, w) plane, it can be seen in Fig. 7 (bottom) that the electromagnetic wave cannot maintain its shape on the optical fiber, as indicated by a shift when propagating.

Fig. 8 represents the dark soliton dynamics in the CQ DNLS equation with $w = 0.36$ fixed and several parameters C in the stable region and varies α. Based on the results obtained in Fig. 8, it is clear that the parameters C and α have an influence on the propagation of electromagnetic waves on fiber optics. The larger the parameters of C, the faster the pulse of electromagnetic waves propagating in the fiber optics will widen. It can be seen in the Fig. 8 that for $C = 0.04$ the pulse widening of the electromagnetic wave starts at $t \approx 350$, then for $C = 0.05$ the pulse widening starts at $t \approx 250$ and for $C = 0.06$ the pulse widening starts at $t \approx 150$. Meanwhile, the α parameter greatly affects the

intensity of the electromagnetic wave, which affects the amplitude height of the electromagnetic wave. The larger the parameters of α, the faster the intensity of the electromagnetic wave decreases.

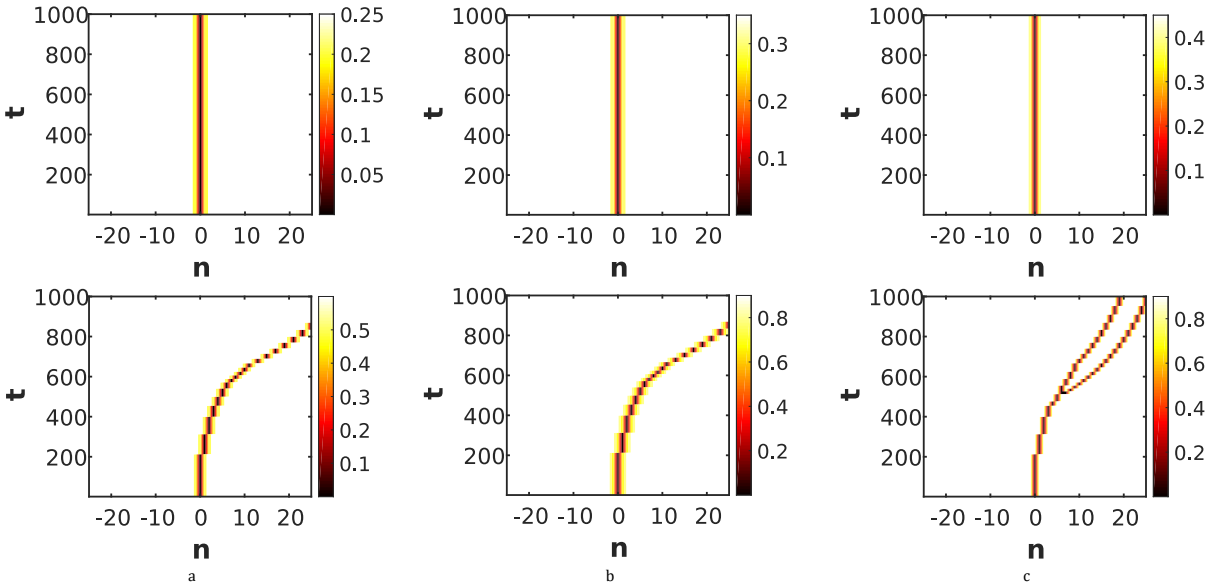

Fig. 7: Dark soliton dynamics in the CQ DNLS equation with C = 0.04 fixed and several parameters w (top) (a) w = 0.23, (b) w = 0.3, (c) w = 0.37 (bottom) (a) w = 0.44, (b) w = 0.51, (c) w = 0.58

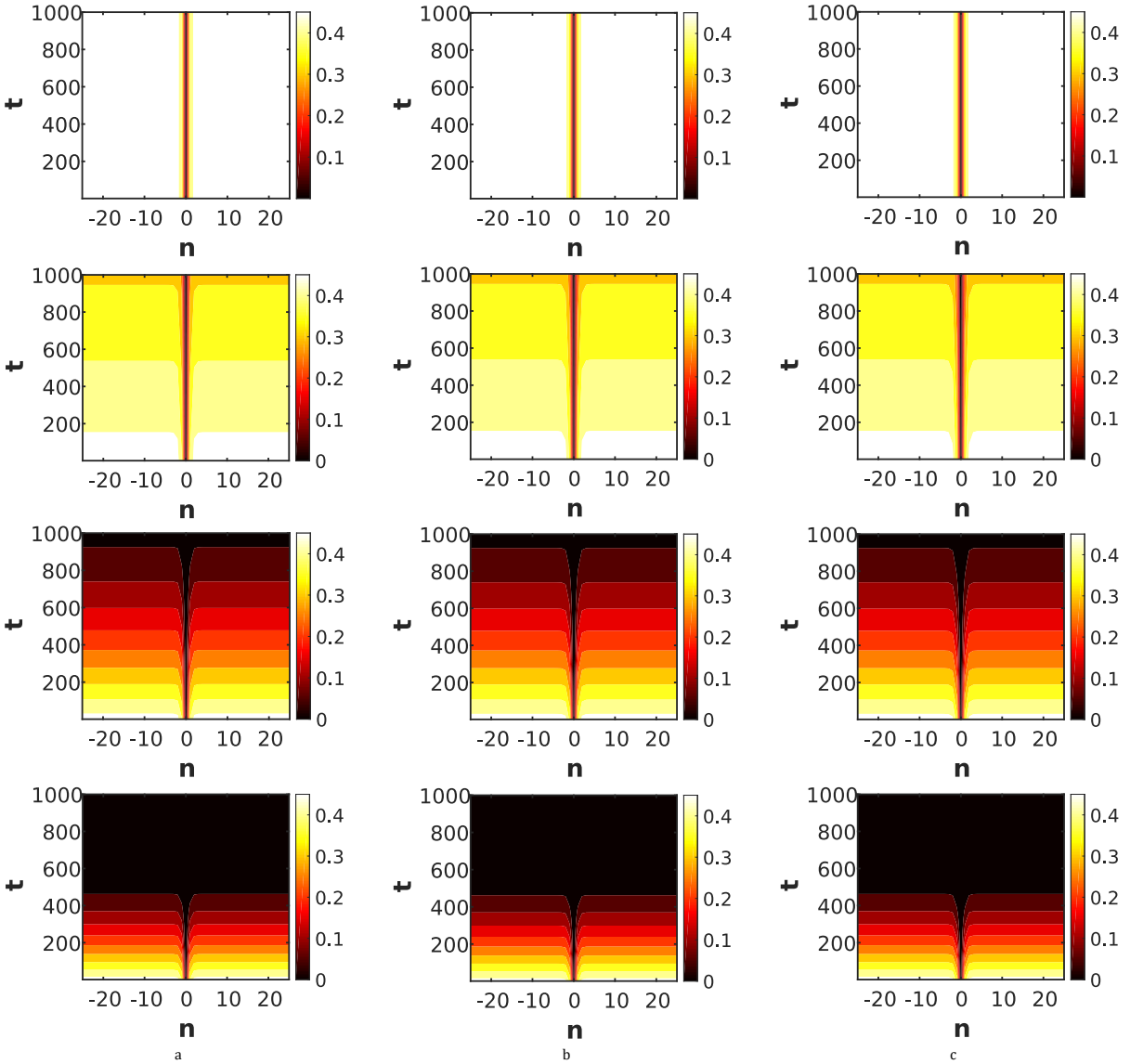

Fig. 8: Dark soliton dynamics in the CQ DNLS equation with w = 0.36 fixed and α = 0 (top), α = 0.01 (row 2), α = 0.05 (row 3) and α = 0.1 (bottom) for several parameters C (a) C = 0.04, (b) C = 0.05, (c) C = 0.06

Fig. 9 represents the dark soliton dynamics in the CQ DNLS equation with $C = 0.04$ fixed and several parameters w in the stable region and varies α. Based on Fig. 9, it can be seen that the parameters w and α have a significant influence on the propagation of electromagnetic waves on the fiber optics. The larger the parameter of w, the greater the amplitude of electromagnetic waves propagating through the fiber optics. Meanwhile, the α parameter influences the intensity of electromagnetic waves propagating through the fiber optics. The greater the value of α, the faster the intensity of electromagnetic waves will decrease. As a result, electromagnetic waves can no longer propagate in the optical fiber.

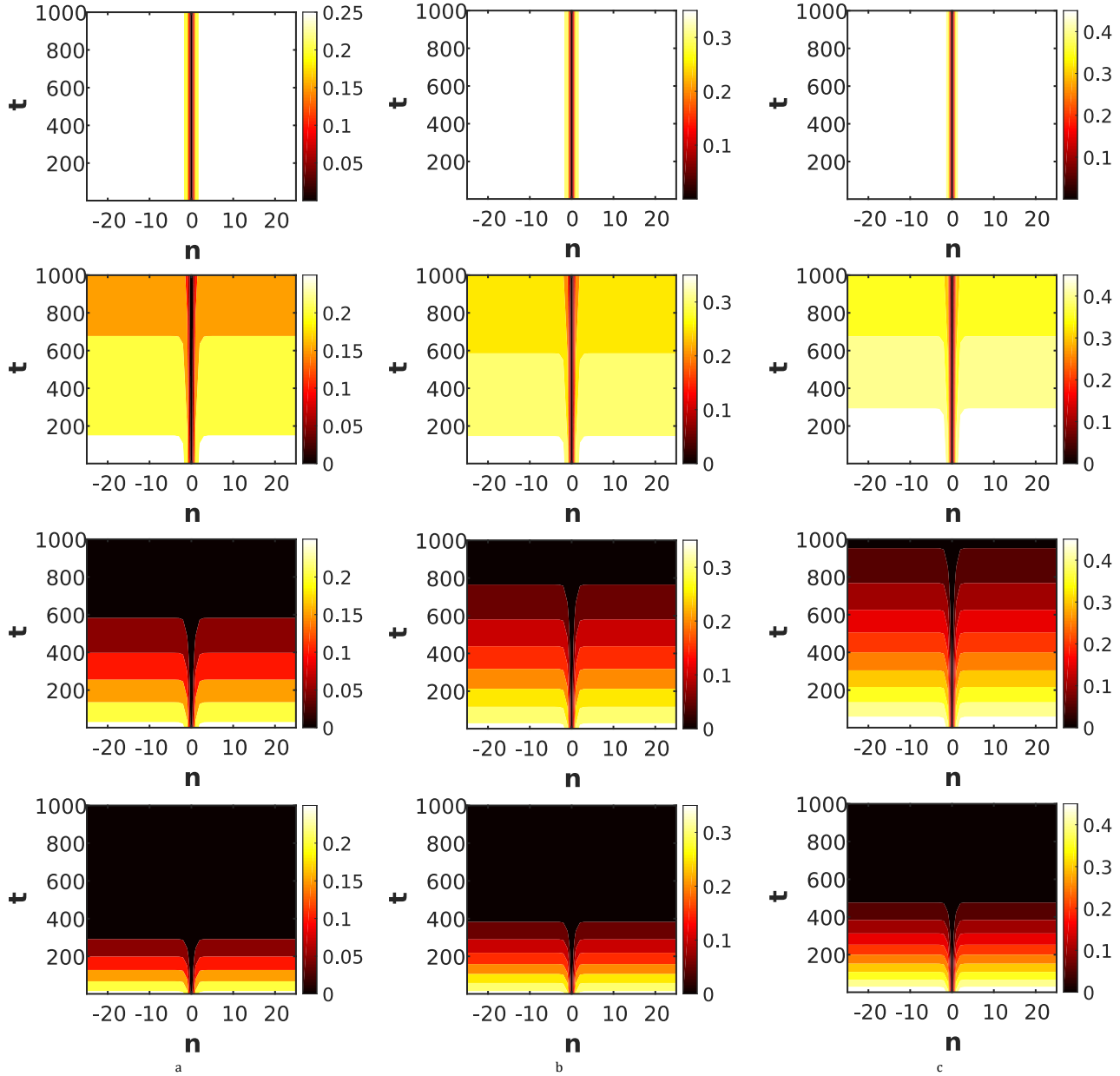

Fig. 9: Dark soliton dynamics in the CQ DNLS equation with C = 0.04 fixed and α = 0 (top), α = 0.01 (row 2), α = 0.05 (row 3) and α = 0.1 (bottom) for several parameters w (a) w = 0.23, (b) w = 0.3, (c) w = 0.37

3.4. Hamiltonian dynamics of cubic-quintic discrete nonlinear Schrödinger's equation

The energy contained in electromagnetic waves propagating in fiber optics can be analyzed by using Hamiltonian dynamics in the CQ DNLS equation. Changes in Hamiltonian dynamics are influenced by several parameters, such as frequency (w), dispersion (C), and attenuation (α).

Fig. 10 represents the Hamiltonian dynamics of the CQ DNLS equation by varying the parameters α, w and C. Hamiltonian dynamics in Fig. 10 (top) is obtained based on dark soliton dynamics in Fig. 8, and Hamiltonian dynamics in Fig. 10 (bottom) is obtained based on dark soliton dynamics in Fig. 9. The energy of electromagnetic waves propagating on fiber optics is described by Hamiltonian dynamics, as shown in Fig. 10.

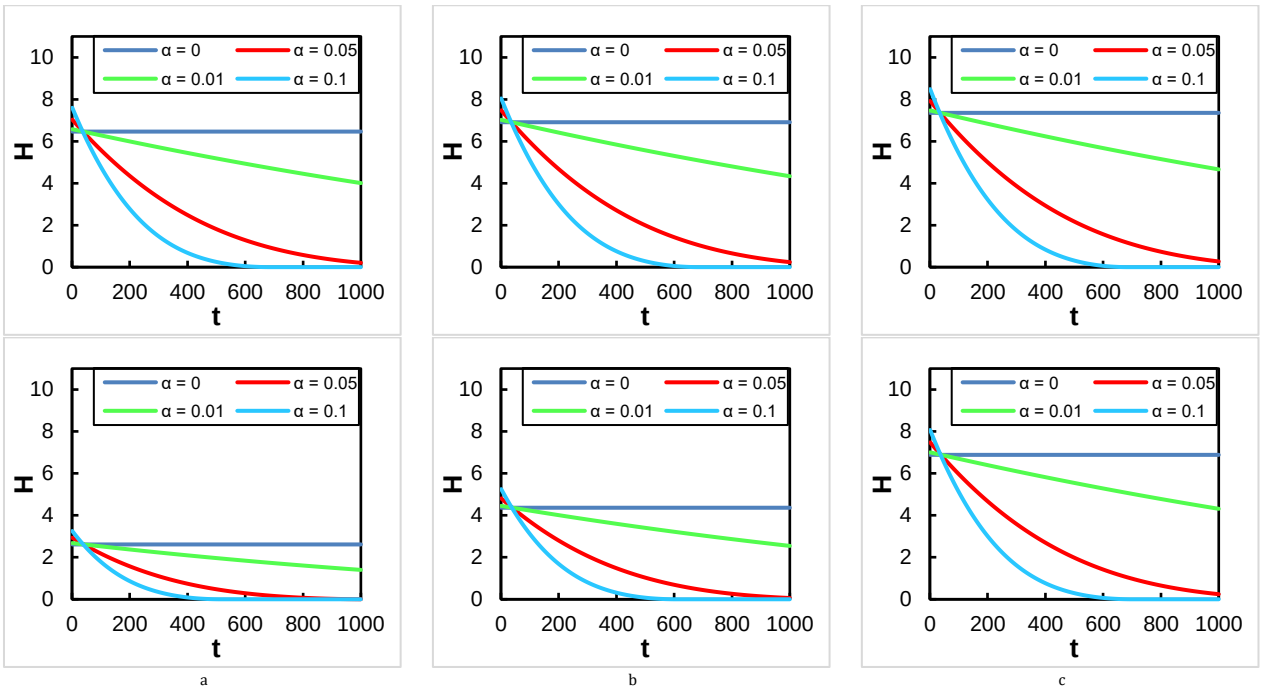

Fig. 10: Hamiltonian dynamics for the CQ DNLS equation for $\alpha = 0, \alpha = 0.01, \alpha = 0.05$ and $\alpha = 0.1$ with (top) parameter $w = 0.36$ fixed with (a) $C = 0.04$, (b) $C = 0.05$, (c) $C = 0.06$ and (bottom) parameter $C = 0.04$ fixed with (a) $w = 0.23$, (b) $w = 0.3$, (c) $w = 0.37$

It is clear that the parameter α has a significant influence on the energy of the electromagnetic wave propagating in the optical fiber. If the parameter α is zero, for a fixed value of C and w, it can be seen that the Hamiltonian value is always constant without loss (marked in blue line). The greater the attenuation effect (α) given, the decrease in energy will be faster. As seen in Fig. 10, in general, the provision of a high attenuation effect (marked in a light blue line) makes electromagnetic waves that propagate on optical fiber experience energy loss faster than others. This is in line with research conducted by Mardi et al. (2023) related to the effect of attenuation on the Hamiltonian Dynamics of Nonlinear Schrodinger equations (Continuos Model). The larger the dispersion effect (C), the wider the pulse of the electromagnetic wave propagating on the fiber optics, resulting in an increase in energy in the wave of electromagnetic. As seen in Fig. 10, the Hamiltonian dynamics with a larger value of C has a greater energy than the others. Meanwhile, the parameter w influences the amplitude of the electromagnetic wave; the greater the frequency value (w) given, the greater the amplitude of the electromagnetic wave propagating in the fiber optics, resulting in an increase in energy in the electromagnetic wave propagating along the fiber optics. The Hamiltonian dynamics with a larger value of w has a greater energy than the others, as seen in Fig. 10.

The findings highlight the importance of understanding and evaluating the effects of dispersion, frequency, and attenuation in materials used for optical fiber cores to optimize electromagnetic wave propagation. To enhance the performance of optical fibers, engineers and researchers must carefully assess the properties of core materials. For example, minimizing impurities in the glass can reduce attenuation, while choosing materials with appropriate refractive indices can mitigate dispersion. Similarly, materials with low absorption coefficients can decrease signal loss due to attenuation, and those with high-frequency response can support faster signal propagation. Further research and development in fiber optics are essential to improve the properties of these materials, enhancing their efficiency and performance in applications such as telecommunications, medical devices, and sensing technologies. Achieving optimal electromagnetic wave propagation requires a comprehensive review of the dispersion, frequency, and attenuation characteristics of the primary material used in optical fiber cores.

4. Conclusion

The dark soliton dynamics and Hamiltonian of the CQ DNLS equation have been analyzed. First, the stationary solution of the CQ DNLS equation is sought, which is required as an input signal to simulate the dark soliton dynamics. The starting point to build the solution is to solve the anti-continuum limit case ($C = 0$). In the case that C is not zero, the stationary solution is sought using the Method of Trust Region Dogleg by taking the starting point $\tanh(n)$ and simulating the values of w and C, resulting in a dark soliton found in the intervals $\in [-0.05,0) \cup (0,0.94]$ and $w \in [0.01,0.89]$. The shape of the dark soliton is affected by changes in the values of the parameters w and C chosen based on these intervals. The smaller parameter of w selected respectively causes an increase in the right sites and a decrease in the left sites, which increases the

height of the dark soliton. In contrast to the parameter w, the increase in the value of parameter C did not cause a change in the height of the dark soliton, only slight changes in position, namely the decrease of sites u_1 and increase of sites u_{-1}. Then, a stability test is carried out on the dark soliton obtained so that the stability region is obtained for the w, C fields. Three points in the stable region and three points in the unstable region are taken to simulate the dynamics of the dark soliton.

Dark soliton dynamics describes the propagation of electromagnetic waves propagating in fiber optics. The dark soliton dynamics are studied using the RK4 Method by taking the stationary solution as the input signal. Based on the results obtained, if the parameters w, C are taken in the unstable region, the electromagnetic wave will experience a shift in its propagation, which ultimately cannot maintain its shape along the optical fiber. Conversely, if the parameter w, C is taken in the stable region, the electromagnetic wave can maintain its shape along the optical fiber. Then by taking the parameters w, C in the stable region, the dark soliton dynamics are simulated by varying the parameter α. Parameters frequency (w), dispersion (C), and attenuation (α) have a significant influence on the propagation of electromagnetic waves on fiber optics. The larger the parameter of w, the higher the amplitude of electromagnetic waves propagating on the fiber optics. The impact of C value on the dynamics of dark soliton is that as C increases, the electromagnetic wave pulse that propagates on the fiber optics widens faster. Finally, the attenuation effect affects electromagnetic wave propagation. The greater the α parameter chosen, the faster the intensity of electromagnetic waves will decrease. These three parameters also have an influence on simulating the dynamics of the Hamiltonian. The Hamiltonian in the CQ DNLS equation examines electromagnetic wave energy propagating through fiber optics. It is found that increasing the values of w and C, each of which affects the increase in amplitude height and widening of the electromagnetic wave, will affect the increase in electromagnetic wave energy when propagating on the optical fiber. Meanwhile, an increase in the value of α, which affects the decrease in electromagnetic wave intensity, causes electromagnetic waves to lose energy as they propagate through the fiber optics.

In summary, achieving maximum electromagnetic wave propagation in optical fibers requires a thorough understanding and evaluation of the effects of dispersion, frequency, and attenuation of materials used to make the cores. Engineers and researchers need to carefully evaluate the properties of the materials used and refine them to optimize the performance and efficiency of optical fibers in various applications. Further research and development in this field can lead to improvements in telecommunications, medical equipment, and sensing technologies. As a result, the primary material used to make optical fiber cores must be reconsidered. To ensure its attenuation, dispersion, and frequency properties are optimized for optimal electromagnetic wave propagation.

List of symbols

arg max	Arguments of the maxima
B	Cubic terms
C	Coupling parameter between two adjacent lattices
$\mathbb{C}$	The set of complex numbers
e	Euler's Number, e = 2,71828 ...
f	Objective function
F	System of nonlinear equations
F_n	The n-th nonlinear equations
H	Hamiltonian
i	Imaginary number, $i = \sqrt{-1}$
J	Jacobian matrix
k	wave number
M_k	Model function at the k-th iteration
m_k	Solution to the model function at the k-th iteration
n	Index
Q	Quintic terms
R_k	Trust region at the k-th iteration
$\mathbb{R}$	The set of real numbers
$\mathbb{R}^+$	The set of positive real numbers
$\mathbb{R}^m$	The set of m-dimentional real numbers
t	Time variable
u	Candidate of soliton solution
u^*	Solution to the unconstrained least squares problem
u_k	Candidate of soliton solution at the k-th iteration
u_n	Elements of a soliton solution candidate
v_{k+1}	Potential candidate of soliton solution at the (k + 1)-th iteration
v_k^c	Cauchy point
v_k^{qn}	Quasi-Newton point
v	Dogleg path
w	Propagation parameter
$\mathbb{Z}$	The set of integer numbers
$\mathbb{Z}^+$	The set of positive integer numbers
	Greek symbols
α	Alpha
α_k^c	Steepest descent direction inside trust region radius at the k-th iteration
α_k^u	Steepest descent direction at the k-th iteration
δ	Delta
τ	Scale that generates part of the dogleg paths
ψ_n	Wave function
$\dot{\psi}_n$	Derivative with respect to time of the wave function
Δ_k	Trust region radius at the k-th iteration
∇	Vector differential operator

Acknowledgment

The authors extend their gratitude to PMDSU Scholarship.

Compliance with ethical standards

Conflict of interest

The author(s) declared no potential conflicts of interest with respect to the research, authorship, and/or publication of this article.

References

Abdel-Gawad HI (2021). Solutions of the generalized transient stimulated Raman scattering equation: Optical pulses compression. Optik, 230: 166314. https://doi.org/10.1016/j.ijleo.2021.166314

Ahmadianfar I, Heidari AA, Gandomi AH, Chu X, and Chen H (2021). RUN beyond the metaphor: An efficient optimization algorithm based on Runge Kutta method. Expert Systems with Applications, 181: 115079. https://doi.org/10.1016/j.eswa.2021.115079

Baronio F, Frisquet B, Chen S, Millot G, Wabnitz S, and Kibler B (2018). Observation of a group of dark rogue waves in a telecommunication optical fiber. Physical Review A, 97(1): 013852. https://doi.org/10.1103/PhysRevA.97.013852

Biondini G and Lottes J (2019). Nonlinear interactions between solitons and dispersive shocks in focusing media. Physical Review E, 99(2): 022215. https://doi.org/10.1103/PhysRevE.99.022215 **PMid:30934274**

Brust JJ, Marcia RF, and Petra CG (2019). Large-scale quasi-Newton trust-region methods with low-dimensional linear equality constraints. Computational Optimization and Applications, 74: 669-701. https://doi.org/10.1007/s10589-019-00127-4

Efe S and Yuce C (2015). Discrete rogue waves in an array of waveguides. Physics Letters, Section A: General, Atomic and Solid State Physics, 379(18-19): 1251-1255. https://doi.org/10.1016/j.physleta.2015.02.031

Gao XY, Guo YJ, and Shan WR (2021). Optical waves/modes in a multicomponent inhomogeneous optical fiber via a three-coupled variable-coefficient nonlinear Schrödinger system. Applied Mathematics Letters, 120: 107161. https://doi.org/10.1016/j.aml.2021.107161

Gninzanlong CL, Ndjomatchoua FT, and Tchawoua C (2018). Discrete breathers dynamic in a model for DNA chain with a finite stacking enthalpy. Chaos: An Interdisciplinary Journal of Nonlinear Science, 28(4): 043105. https://doi.org/10.1063/1.5009147 **PMid:31906659**

Hosseini K, Mirzazadeh M, Baleanu D, Salahshour S, and Akinyemi L (2022). Optical solitons of a high-order nonlinear Schrödinger equation involving nonlinear dispersions and Kerr effect. Optical and Quantum Electronics, 54: 177. https://doi.org/10.1007/s11082-022-03522-0

Jia Q, Qiu H, and Mateo AM (2022). Soliton collisions in Bose-Einstein condensates with current-dependent interactions. Physical Review A, 106(6): 063314. https://doi.org/10.1103/PhysRevA.106.063314

Kartono A, Fatmawati VW, and Wahyudi ST (2020). Numerical solution of nonlinear Schrodinger approaches using the fourth-order Runge-Kutta method for predicting stock pricing. Journal of Physics: Conference Series, 1491: 012021. https://doi.org/10.1088/1742-6596/1491/1/012021

Kevrekidis PG (2009). The discrete nonlinear Schrödinger equation: Mathematical analysis, numerical computations and physical perspectives. Volume 232, Springer Science and Business Media, Berlin, Germany. https://doi.org/10.1007/978-3-540-89199-4

Kevrekidis PG and Carretero-González R (2009). A map approach to stationary solutions of the DNLS equation. In: Kevrekidis PG (Ed.), The discrete nonlinear schrödinger equation: Mathematical analysis, numerical computations and physical perspectives: 221-233. Volume 232, Springer Science and Business Media, Berlin, Germany. https://doi.org/10.1007/978-3-540-89199-4_11

Kimiaei M (2022). An active set trust-region method for bound-constrained optimization. Bulletin of the Iranian Mathematical Society, 48: 1721-1745. https://doi.org/10.1007/s41980-021-00610-x

Kourakis I and Shukla PK (2005). Discrete breather modes associated with vertical dust grain oscillations in dusty plasma crystals. Physics of Plasmas, 12(1): 014502. https://doi.org/10.1063/1.1824908

Liu X, Luan Z, Zhou Q, Liu W, and Biswas A (2019). Dark two-soliton solutions for nonlinear Schrödinger equations in inhomogeneous optical fibers. Chinese Journal of Physics, 61: 310-315. https://doi.org/10.1016/j.cjph.2019.08.006

Maluckov A, Hadžievski L, and Malomed BA (2007). Dark solitons in dynamical lattices with the cubic-quintic nonlinearity. Physical Review E, 76(4): 046605. https://doi.org/10.1103/PhysRevE.76.046605 **PMid:17995125**

Mardi HA, Nasaruddin N, Ikhwan M, Nurmaulidar N, and Ramli M (2023). Soliton dynamics in optical fiber based on nonlinear Schrödinger equation. Heliyon, 9: e14235. https://doi.org/10.1016/j.heliyon.2023.e14235 **PMid:36942232 PMCid:PMC10024108**

Motcheyo ABT, Kimura M, Doi Y, and Tchawoua C (2019). Supratransmission in discrete one-dimensional lattices with the cubic–quintic nonlinearity. Nonlinear Dynamics, 95: 2461-2468. https://doi.org/10.1007/s11071-018-4707-y

Motcheyo ABT, Tchawoua C, Siewe MS, and Tchameu JDT (2011). Multisolitons and stability of two hump solitons of upper cutoff mode in discrete electrical transmission line. Physics Letters A, 375(7): 1104-1109. https://doi.org/10.1016/j.physleta.2011.01.018

Motcheyo AT and Macías-Díaz JE (2023). Nonlinear bandgap transmission with zero frequency in a cross-stitch lattice. Chaos, Solitons and Fractals, 170: 113349. https://doi.org/10.1016/j.chaos.2023.113349

Motcheyo AT, Tchameu JT, Siewe MS, and Tchawoua C (2017). Homoclinic nonlinear band gap transmission threshold in discrete optical waveguide arrays. Communications in Nonlinear Science and Numerical Simulation, 50: 29-34. https://doi.org/10.1016/j.cnsns.2017.02.001

Okaly JB and Nkoa NT (2022). Nonlinear dynamics of DNA chain with long-range interactions. In: Zdravković S and Chevizovich D (Eds.), Nonlinear dynamics of nanobiophysics: 67-96. Springer Nature, Singapore, Singapore. https://doi.org/10.1007/978-981-19-5323-1_4

Ozisik M (2022). On the optical soliton solution of the (1+ 1) − dimensional perturbed NLSE in optical nano-fibers. Optik, 250: 168233. https://doi.org/10.1016/j.ijleo.2021.168233

Qausar H, Ramli M, Munzir S, Syafwan M, Susanto H, and Halfiani V (2020). Nontrivial on-site soliton solutions for stationary cubic-quintic discrete nonlinear Schrodinger equation. IAENG International Journal of Applied Mathematics, 50(2): 1-5. https://doi.org/10.2139/ssrn.3901859

Qi Y, Yang S, Wang J, Li L, Bai Z, Wang Y, and Lv Z (2022). Recent advance of emerging low-dimensional materials for vector soliton generation in fiber lasers. Materials Today Physics, 23: 100622. https://doi.org/10.1016/j.mtphys.2022.100622

Raza N, Hassan Z, and Seadawy A (2021). Computational soliton solutions for the variable coefficient nonlinear Schrödinger equation by collective variable method. Optical and Quantum Electronics, 53: 400. https://doi.org/10.1007/s11082-021-03052-1

Song Y, Shi X, Wu C, Tang D, and Zhang H (2019). Recent progress of study on optical solitons in fiber lasers. Applied Physics Reviews, 6(2): 021313. https://doi.org/10.1063/1.5091811

Susanto H and Karjanto N (2008). Calculated threshold of supratransmission phenomena in waveguide arrays with saturable nonlinearity. Journal of Nonlinear Optical Physics and Materials, 17(02): 159-165. https://doi.org/10.1142/S0218863508004147

Syafwan M and Arifin N (2018). Variational approximations for twisted solitons in a parametrically driven discrete nonlinear Schrödinger equation. Journal of Physics: Conference Series,

983(1): 012145. https://doi.org/10.1088/1742-6596/983/1/012145

Tang D, Guo J, Song Y, Zhang H, Zhao L, and Shen D (2014). Dark soliton fiber lasers. Optics Express, 22(16): 19831-19837. https://doi.org/10.1364/OE.22.019831 **PMid:25321066**

Wang C, Nie Z, Xie W, Gao J, Zhou Q, and Liu W (2019). Dark soliton control based on dispersion and nonlinearity for third-order nonlinear Schrödinger equation. Optik, 184: 370-376. https://doi.org/10.1016/j.ijleo.2019.04.020

Wang L, Luan Z, Zhou Q, Biswas A, Alzahrani AK, and Liu W (2021). Effects of dispersion terms on optical soliton propagation in a lossy fiber system. Nonlinear Dynamics, 104: 629-637. https://doi.org/10.1007/s11071-021-06283-9

Wang S, Ma G, Zhang X, and Zhu D (2022). Dynamic behavior of optical soliton interactions in optical communication systems. Chinese Physics Letters, 39(11): 114202. https://doi.org/10.1088/0256-307X/39/11/114202

Wang X, Ding X, and Qu Q (2020). A new nonmonotone adaptive trust region line search method for unconstrained optimization. Journal of Mathematics in Industry, 10: 13. https://doi.org/10.1186/s13362-020-00080-6

Yan XW and Chen Y (2022). Soliton interaction of a generalized nonlinear Schrödinger equation in an optical fiber. Applied Mathematics Letters, 125: 107737. https://doi.org/10.1016/j.aml.2021.107737

Yang S, Zhang QY, Zhu ZW, Qi YY, Yin P, Ge YQ, and Zhang H (2022). Recent advances and challenges on dark solitons in fiber lasers. Optics and Laser Technology, 152: 108116. https://doi.org/10.1016/j.optlastec.2022.108116

Yao Y, Ma G, Zhang X, and Liu W (2019). M-typed dark soliton generation in optical fibers. Optik, 193: 162997. https://doi.org/10.1016/j.ijleo.2019.162997

Zanga D, Fewo SI, Tabi CB, and Kofané TC (2020). Modulational instability in weak nonlocal nonlinear media with competing Kerr and non-Kerr nonlinearities. Communications in Nonlinear Science and Numerical Simulation, 80: 104993. https://doi.org/10.1016/j.cnsns.2019.104993

Zhang AX, Hu XW, Zhang W, Liang JC, and Xue JK (2022). Nonlinear dynamics of tunable spin-orbit coupled Bose-Einstein condensates in deep optical lattices. Physics Letters A, 456: 128529. https://doi.org/10.1016/j.physleta.2022.128529

Zhao J, Luan Z, Zhang P, Dai C, Biswas A, Liu W, and Kudryashov NA (2020). Dark three-soliton for a nonlinear Schrödinger equation in inhomogeneous optical fiber. Optik, 220: 165189. https://doi.org/10.1016/j.ijleo.2020.165189

Zhao XH and Li S (2022). Dark soliton solutions for a variable coefficient higher-order Schrödinger equation in the dispersion decreasing fibers. Applied Mathematics Letters, 132: 108159. https://doi.org/10.1016/j.aml.2022.108159